CCS Chemistry

RESEARCH ARTICLE

Received: Feb. 14, 2018 | Accepted: May 5, 2019 | Published: Sept. 9, 2019

Imine-Rich Poly(*o*-phenylenediamine) as High-Capacity Trifunctional Organic Electrode for Alkali-Ion Batteries

Tao Sun[1,2], Zong-Jun Li[3], Xu Yang[1], Sai Wang[1], Yun-Hai Zhu[1] & Xin-Bo Zhang[1]*

[1]*State Key Laboratory of Rare Earth Resource Utilization, Changchun Institute of Applied Chemistry, Chinese Academy of Sciences, Changchun 130022 (China),* [2]*University of Chinese Academy of Sciences, Beijing 100049 (China),* [3]*State Key Laboratory of Electroanalytical Chemistry, Changchun Institute of Applied Chemistry, Chinese Academy of Sciences, Changchun 130022 (China)*

**Corresponding author: xbzhang@ciac.ac.cn*

Cite this: *CCS Chem.* **2019**, *1*, 365–372

Alkali-ion batteries, including potassium-ion batteries, lithium-ion batteries, and sodium-ion batteries are important energy storage devices; however, with the cation size increased, there exists a great challenge for an inorganic electrode material to accommodate the different properties of the alkali-ion. Herein, as a proof-of-concept experiment, an imine-rich poly(*o*-phenylenediamine) (PoPD) is synthesized through a rational controllable oxidization. Due to the abundance of active sites and ladder-conjugated structure, PoPD in the optimized oxidation state endows alkali-ion batteries with a stable cyclability at high capacity. The highly reversible redox performance of PoPD with alkali-ions is verified by theoretical calculations and demonstrated as a trifunctional electrode material (537 and 307 mAh·g^{-1} for Li and Na storage capacity after 300 cycles, respectively), especially for successful application in potassium storage (450 mAh·g^{-1} after 205 cycles), and provides compelling evidence for the wide application of organic electrode materials.

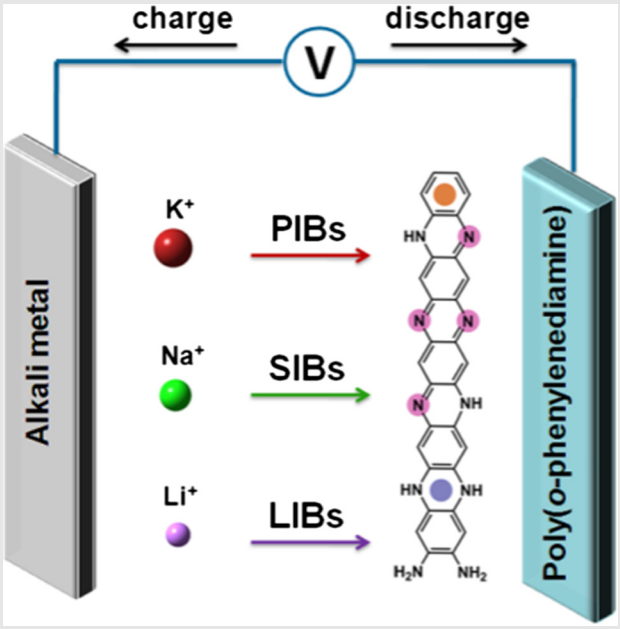

Keywords: potassium-ion batteries, organic electrode, poly(*o*-phenylenediamine), lithium-ion batteries, sodium-ion batteries

DOI: 10.31635/ccschem.019.20190003
CCS Chem. **2019**, *1*, 365–372

Introduction

In the past decades, batteries based on the reversible storage of alkali-ions have achieved great success. Among them, lithium-ion batteries (LIBs) have brought great convenience to our daily lives; however, their development still lags behind the requirements for sustainable energy storage devices.[1,2] To solve the scarcity and uneven distribution of Li, the nonlithium battery systems based on alternative alkali metals ions, such as sodium-ion batteries (SIBs) and potassium-ion batteries (PIBs), have attracted great attention due to their Earth-abundant mineral resource requirements and similar operation principle as LIBs.[3–5] Theoretically, the reduction potential of K^+/K (–2.93 V) is close to Li^+/Li (–3.04 V), which is even lower than its Na counterpart (–2.71 V), and yields PIBs with high voltage and energy.[6–8] However, the large-scale applications of PIBs are still facing many challenges, including relative low capacity and bad cycling stability.[9–12] Due to the large size of K ions, an inorganic electrode based on intercalation or an alloying reaction is often associated with drastic structural changes during the electrochemical cycling, which will deteriorate its performances.[13–17] As a matter of fact, this phenomenon is not only limited to PIBs. As is well known, even though PIBs share a similar energy storage mechanism to that of their Li counterparts, similar inorganic materials that are widely used in LIBs cannot be successfully used in SIBs or in PIBs. Each type of alkali-ion requires a unique crystal structure and insertable sites. Restricted by the rigid structure, it is an almost impossible task to find a suitable inorganic electrode material for the reversible storage and release of alkali-ions with different properties. Increasing the size of the alkali-ion presents a great challenge for traditional inorganic electrode materials.

Interestingly, an organic compound is a promising candidate for the intercalation of large metal ions.[18–21] Assembled by the van der Waals force, an organic compound featuring a large spacing and flexible structure provides an elastic buffer matrix to accommodate the volume expansion/contraction during the K ion insertion/extraction process. However, the dissolution of small molecular material in the electrolyte is a serious problem, which severely disrupts its cycling stability. To overcome this issue, an efficient strategy is to construct a high-performance polymer electrode material with a stable skeleton and abundant electroactive groups.[22]

Among various redox-active polymers, poly(*o*-phenylenediamine) (PoPD), characterized by a highly reversible redox chemistry and unique doping mechanism, has attracted a great deal of attention in the electrochemistry field.[23–25] In fact, the abundant nitrogen-containing functional groups and ladder-conjugated structures would endow PoPD with a high capacity and stable reversibility, and it would thus potentially form a good candidate electrode material. Importantly, the flexible host polymer matrix allows for frequent intercalation and deintercalation of K ions, which avoids the worry of volume change. The working principle of the organic material is based on the redox reaction of the functional group accompanied by the incorporation/release of alkali metal ions or electrolyte anions.[1] To a certain extent, organic materials are not typically restricted by the choice of counter-ion, which indicates that the same organic material is practicable for different energy storage devices.[26–28] Therefore, it could be predicted that PoPD is a versatile electrode, wherein K^+, Na^+, and Li^+ could offer reversible storage and release.

Doping state is a crucial factor determining the properties of an aromatic amine polymer.[24,26] Therefore, to obtain satisfactory electrochemical performance, the oxidation state of PoPD should be rationally designed. Quinoid imine (–N=) unit is a characteristic of the oxidation state of PoPD, which is also the major active site to bond with alkali metal ions. A greater quinoid imine content in PoPD means more active sites and better electrochemical performance; however, excessive oxidation will deteriorate the electronic conductivity and stability.[26] Accordingly, oxidation state optimization is crucial for PoPD to exhibit the optimized electrochemical properties, but to achieve this remains challenging.

Herein, PoPD with a variable oxidation state is synthesized as a trifunctional electrode for alkali-ion batteries. Taking the potassium storage performance as an example, through a rational manipulation of oxidant in the synthesis procedure, the relationship between oxidation state and electrochemical behavior is investigated. Due to the abundance of active sites, PoPD in the optimized oxidation state exhibits excellent PIB performance, including a high specific capacity and cycling stability (450 $mAh{\cdot}g^{-1}$ after 205 cycles). As a versatile electrode, PoPD also exhibits a reversible capacity of 537 and 307 $mAh{\cdot}g^{-1}$ for LIBs and SIBs, respectively, which offer convincing evidence for the great potential application of organic electrode materials.

Results and Discussion

Poly(*o*-phenylenediamine was synthesized through chemical oxidative polymerization using ammonium persulfate (APS) [$(NH_4)_2S_2O_8$] as oxidant (Figure 1a).[25] To tune the degree of oxidation and electrochemical performance, a series of samples with APS/*o*PD ratios varying from 0.5:1 to 3:1 have been fabricated, which were labeled PoPD-0.5 to PoPD-3, respectively (Supporting Information Figure S2). Fourier-transform infrared spectroscopy (FTIR) clearly demonstrates the formation of PoPD (Figure 1b). The stretching vibration of the quinoid ring is found at 1618 cm^{-1}. Two signals at 1350

DOI: 10.31635/ccschem.019.20190003
CCS Chem. **2019**, *1*, 365–372

and 1221 cm^{-1} correspond to the C–N stretch mode in the quinoid and benzenoid rings, respectively. The band at 850 cm^{-1} can be assigned to the C–H out-of-plane bending vibration of the 1,2,4,5-tetrasubstituted benzenoid, indicating the existence of a rigid phenazine skeleton in PoPD. However, the peak located at 1134 cm^{-1} corresponds to the in-plane bending vibrations of the 1,2,4-trisubstituted benzenoid, suggesting the PoPD does not have a perfect ladder structure. Therefore, it can be concluded that the as-prepared PoPD has a rigid skeleton with some open rings.[25] With increasing oxidant/monomer ratio, the stretching of the quinoid ring at 1618 cm^{-1} is increased, but the signal at 1517 cm^{-1} (benzenoid ring) becomes weaker and even disappears when the ratio reaches 3:1, which indicates an decreased benzenoid content but increased quinoid content. Accordingly, the oxidation state of PoPD improves as the amount of oxidant increased.

This conclusion can also be demonstrated by the elucidation of the N1s spectra of PoPD. According to the X-ray photoelectron spectroscopy (XPS) (Figure 1c and Supporting Information Figure S1 and Table S1), the peak of the N1s spectra can be fitted with three components: –N=, –NH–, and $–NH_2$, which are centered at 398.1, 399.2, and 400.2 eV, respectively. For the PoPD-0.5, the content of quinoid imine is 34.8%, whereas for PoPD-3, this value increased to 58% (Supporting Information Table S1). The reduced benzenoid amine content means the benzenoid amine has been oxidized to quinoid imine, thus yielding a PoPD sample in high oxidation state. Generally, the area ratio of imine to amine peaks (–N=/–NH–) can be used to determine the oxidation state of aromatic amine/diamine polymers. As the XPS analysis results shown in Figure 1c, it is obvious that the ratio of imine to amine is improved as the oxidant/monomer ratio is increased, which substantiates the assumption that the proportion of imine increases as the oxidation state increases. However, it does not imply that a higher oxidation state presents a better electrochemical performance.

Through the comparison of the cycling performance of different PoPD samples, the effect of oxidation state on electrochemical performance can be clearly demonstrated (Figure 2a and Supporting Information Figure S3). For the samples in a low oxidation state, PoPD-0.5 nearly cannot deliver any capacity. Unexpectedly, PoPD exhibited excellent potassium storage performance when the molar ratio increased to 1:1. The capacity of PoPD-1 achieved 147 $mAh·g^{-1}$ in the first cycle and increased gradually in the following 50 cycles. During the next 70 cycles, the reversible capacity of PoPD-1 became stable and reached 240 $mAh·g^{-1}$. Even the discharge capacity of PoPD-2 reached 253 $mAh·g^{-1}$ in the first cycle; however, this remarkable value decreased upon cycling and was maintained at 150 $mAh·g^{-1}$ after 120 cycles. On increasing the molar ratio to 3:1, there was a decrease in the capacity. A reasonable oxidation state is critical for the aromatic amine/diamine polymers to exhibit the optimized electrochemical activity. Because of the repulsion of charge between structural units, the excessive oxidation state is unstable and usually involves side reactions with the electrolyte. Therefore, 1:1 is the optimized molar ratio, wherein PoPD electrodes exhibit the optimized electrochemical performance.

Figure 2c shows the discharge/charge curves of the 1st, 2nd, 10th, and 100th cycle for the PoPD-1 electrode at 50 $mA·g^{-1}$. The large capacity gap between the initial

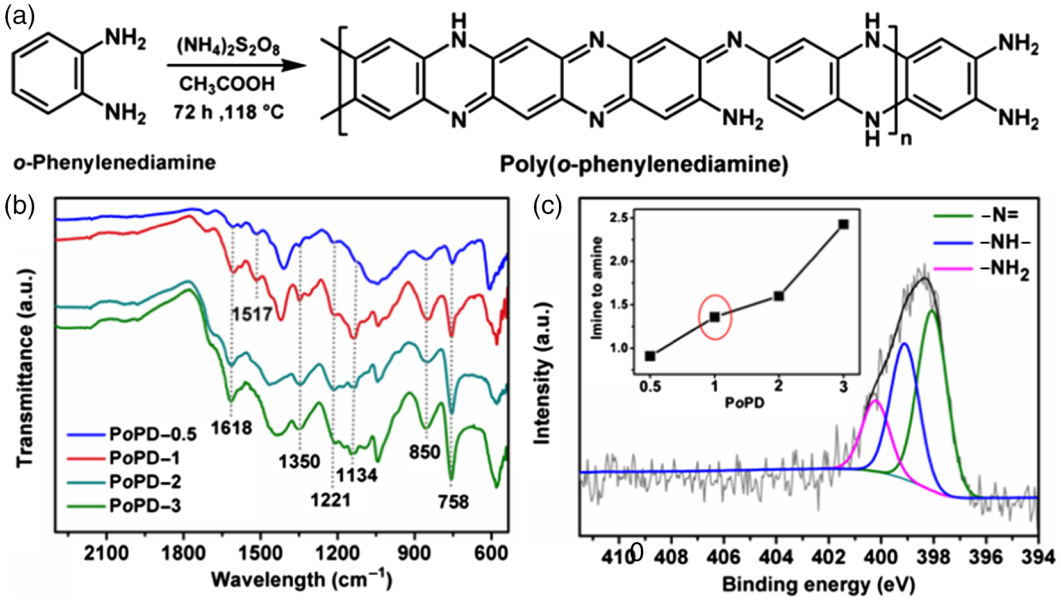

Figure 1 | *Preparation and characterization of PoPD. (a) Synthesis of PoPD. (b) FTIR of PoPD samples. (c) XPS spectrum of PoPD.*

DOI: 10.31635/ccschem.019.20190003
CCS Chem. **2019**, *1*, 365–372

discharge and the next charge process corresponds to the formation of a solid electrolyte interphase layer. When tested at 50 mA·g^{-1}, the reversible capacity of PoPD-1 reached 450 mAh·g^{-1} after which it became stable from the 100th cycle and continued to sustain this high capacity for the next 105 cycles (Figure 2b). Such a high capacity and cycling stability are rarely seen in PIBs or in organic electrode materials even without using any special carbon-based composite techniques (Supporting Information Table S5). For PoPD-1, it should be noted that there exists an activation process during the cycling process (Figure 2a,b). On the one hand, due to the insufficient contact between the polymer and the electrolyte, the capacity increasing stage can be identified as an "activation process."[29] On the other hand, this phenomenon might probably be attributed to the oxidation of benzenoid amine to quinoid imine during charge/discharge process. In other words, the cycling process will improve the efficiency of redox reactions and expose more active sites.[26] Excepting the high capacity, the rate capability of PoPD-1 was further investigated under various test conditions. As displayed in Figure 2d, PoPD-1 delivers a stable capacity of 313, 227, 149, 104, and 73 mAh·g^{-1} at different current rates of 100, 200, 500, 1000, and 2000 mA·g^{-1}, respectively. When the current rate returned to 50 mA·g^{-1}, the PoPD-1 electrode recovered a reversible capacity of 300 mAh·g^{-1}.

To gain insight into the energy storage mechanism of PoPD, density functional theory (DFT) calculations were applied to discuss the reaction process from the aspects of reaction kinetics and thermodynamics (Figure 3). To simplify the calculation, the project was initiated by designing a core structure of PoPD, which only contains benzenoid amine and quinoid imine. First, natural bond orbital (NBO) charge distributions are performed to analyze the process of potassium insertion (Supporting Information Figure S5). When the PoPD is reduced to monoanion PoPD^{-}, the negative charge on quinoid imine nitrogen (N18 and N19) increased greatly (from −0.484 to −0.607) (Supporting Information Figure S6). When the first potassium was inserted, imine nitrogen (N18) and potassium possess the most negative (−0.730) and positive charges (0.937), which indicates the formation of a chemical bond. On receipt of the second electron, the N19 atom showed the greatest increase of negative charge in monoanion PoPD-1K^{-} (Supporting Information Figure S6). Therefore, an N19 atom would be the most active site to bind with the second potassium. Based on the above analysis, it can be deduced that imine nitrogen is the most active site to bind with K, and this reflects the importance of imine (C=N bond) in PoPD. This conclusion is supported by the thermodynamics calculations, wherein the negative stabilization energy value indicates a favorable binding of the potassium ions (Figure 3c and

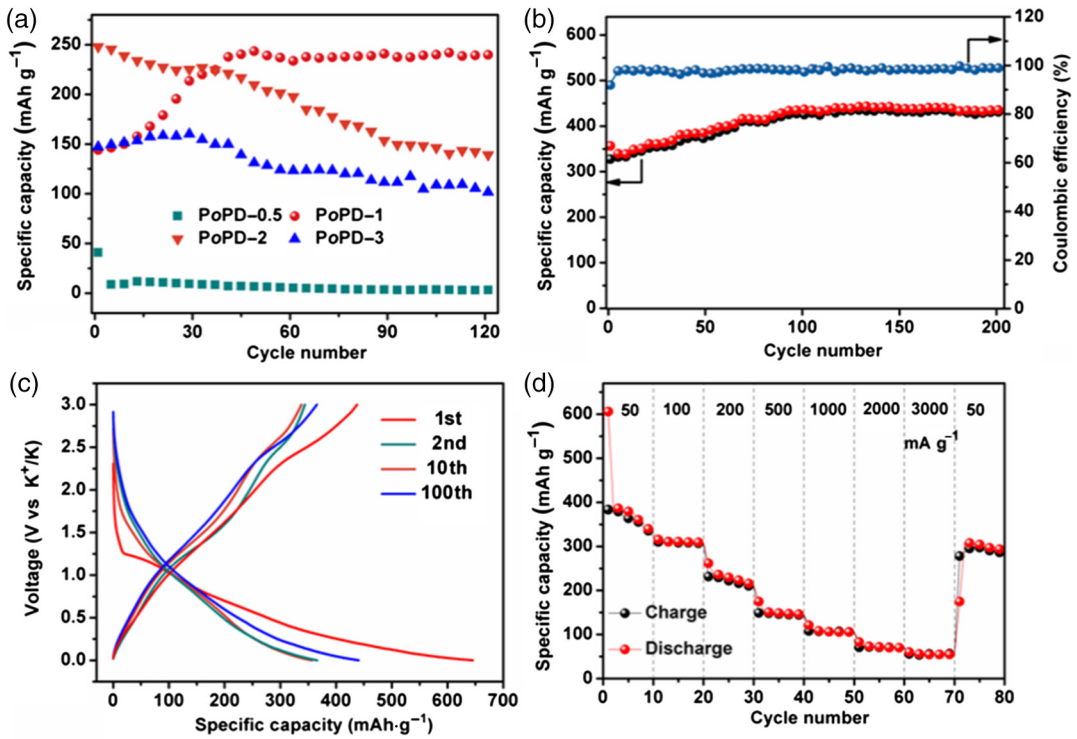

Figure 2 | *Electrochemical performance of PoPD as PIBs anode. (a) Cycling performance comparison of PoPD samples (charge capacity profiles vs cycle number under a current of 200 mA·g^{-1}). (b) Cycling performance of PoPD-1. (c) Discharge/charge profiles of PoPD-1. (d) Rate performance of PoPD-1.*

DOI: 10.31635/ccschem.019.20190003
CCS Chem. **2019**, *1*, 365–372

Supporting Information Table S2). It is worth noting that the binding energy of the second potassium (−0.75 eV) is stronger than the first one (−0.50 eV), which indicates that the insertion of the first potassium facilitates the second step.

During the stepwise redox process of PoPD, the evolution of the conjugated structure is clearly manifested by the changes in the major bond lengths (Figure 3b and Supporting Information Figure S7). With the aid of a ladder-conjugated system, the homogenization of bond length occurs, wherein the distinct length gap between double bond and single bond gradually decreased during the process of potassium insertion.[30,31] In the process of reduction, the π-conjugated skeleton could effectively delocalize the negative charge, and thus achieve the stabilization of the reduced PoPD. The length of the C=N double bond is increased as the reduction process; in the fully reduced state, the length gap between the C=N (C7–N19 and C2–N18) and C–N (C1–N18 and C10–N19) bonds reaches a minimum, which implies the consumption of the C=N bond and is consistent with the above NBO charge analysis.

The ladder-conjugated skeleton plays a significant role in determining the electrochemical performance of PoPD, in which the electron transfer not only will be easier, but also presents a stable backbone that can tolerate frequent redox in the discharge/charge process. More importantly, the rigid ladder-conjugated structures can also provide the potential binding active sites to storage K ions, except the C=N bond. In fact, structures of benzene and pyrazine are also strong binding sites for the electron-deficient K cations, which can be attributed to the interaction of potassium with the π electrons.[30,32] Supporting Information Figure S8 presents the NBO charge distributions in the complexes of PoPD and potassium, wherein the potassium atom above the plane of the benzene ring and phenazine ring bearing the largest positive charge densities (0.957 and 0.943) are shown, indicating the strong interaction between potassium and six-membered rings. The distance of the centroid of the benzene ring and potassium is around at 2.672 Å, which is similar to the length of the K–N bond (Figure 3d,f). However, this distance is shortened to 2.585 Å when potassium is placed above the plane of the phenazine

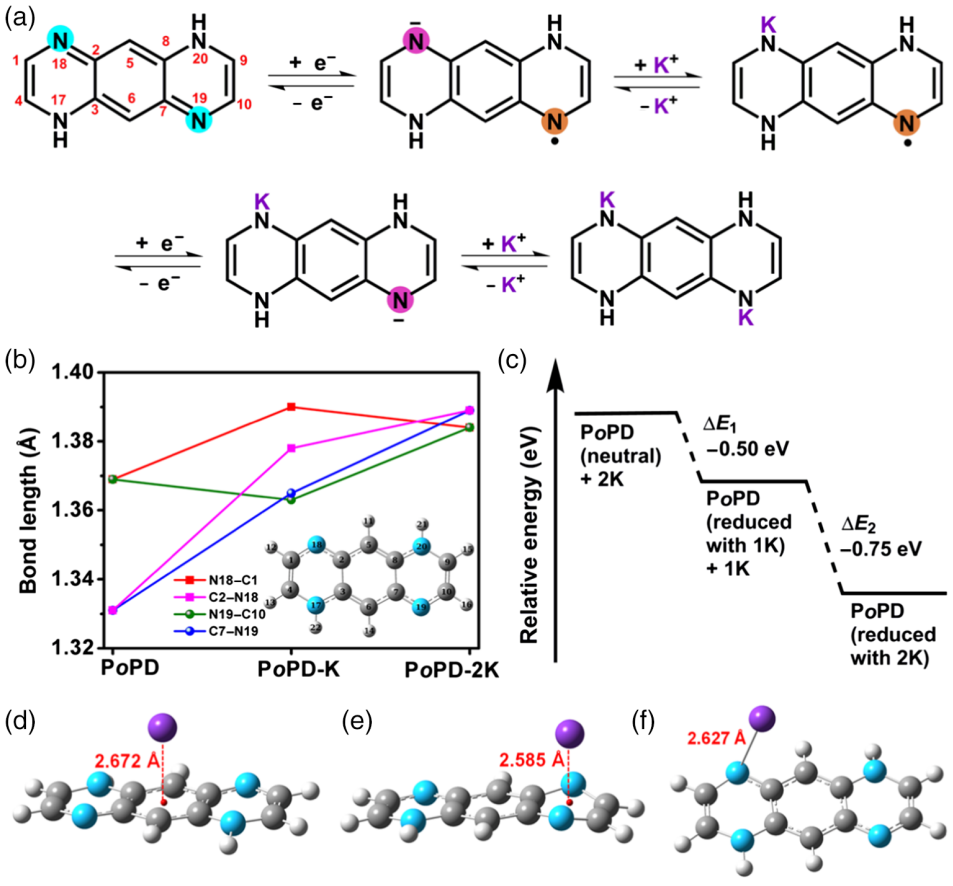

Figure 3 | *DFT calculations and redox mechanism. (a) Electrochemical redox process of PoPD. (b) Major bond length change of PoPD during the reduction process. (c) Stabilization energies at various reduction stages of PoPD. (d–f) Three configurations of PoPD-K.*

DOI: 10.31635/ccschem.019.20190003
CCS Chem. **2019**, *1*, 365–372

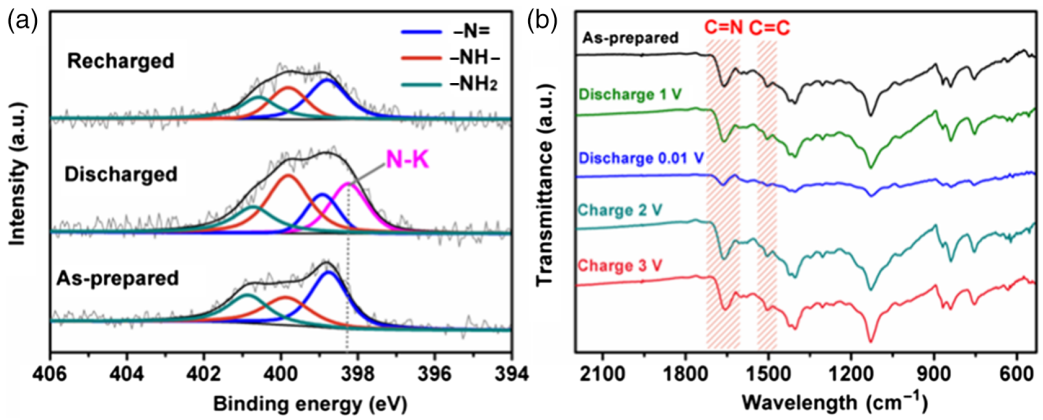

Figure 4 | *Ex situ analysis of PoPD-1 electrode at different states. (a) Ex situ XPS local scan spectra of N1s regions. (b) Ex-situ FTIR characterizations.*

ring (Figure 3e), in which the most negative charge in the N19 and N20 atoms (−0.711 and −0.724) would exhibit a strong interaction with the potassium (Supporting Information Figure S8). Based on above discussion, it can be concluded that PoPD is a promising electrode material for KIBs due to its diversified energy storage mechanism and abundant active sites.

To investigate the structural change of PoPD at different stages of electrochemical reactions and to verify the theoretical studies, ex situ XPS analysis was performed (Figure 4a). For the fresh electrode, the characteristic peaks are in good accordance with the spectra of pristine PoPD. After being discharged to 0.01 V, the peak located at 398.6 eV (–N=) weakens, indicating the consumption of imine. Meanwhile, a new peak centered at 286.6 eV emerges, which implies the formation of a new bond between potassium and nitrogen (K–N). Recharged to 3.0 V, the K–N bond disappeared; all the peaks recovered to the pristine state. The reversible change of the imine vibration mode strongly supports the participation of imine in the reversible reaction with potassium. This conclusion gains support from the ex situ FTIR spectroscopy (Figure 4b), in which the stretching vibration of the quinoid ring located at 1665 cm^{-1} gradually weakens during the reduction process. The stretching vibrations of the C=C bond at 1505 cm^{-1} nearly disappeared in the discharged state, suggesting the reaction of the benzene ring and potassium. In the charge process, these peaks appear reversibly. In addition, the repeatability of the FTIR spectral signals in other regions also provides compelling evidence for the participation of the entire PoPD during the discharge/charge process.

As mentioned above, the working principle of PoPD is based on the redox reaction of the functional group and is not typically restricted by the choice of counter-ion, which implies that PoPD can also be used as an electrode material for SIBs and LIBs. Fortunately, this assumption is demonstrated by the theoretical analysis, in which the stabilization energy profiles and bond length change explicitly demonstrate that the PoPD is also suitable to

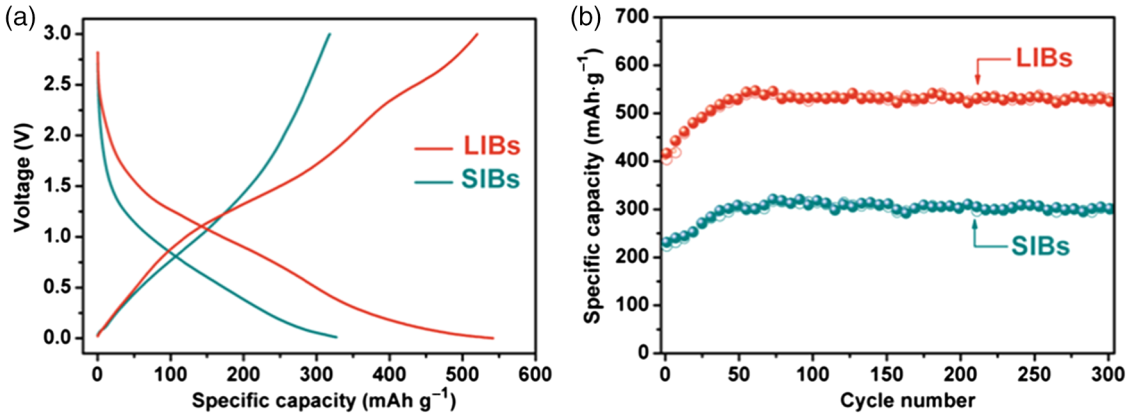

Figure 5 | *Electrochemical performance of PoPD-1 as LIBs and SIBs anode at a current density of 500 mA·g^{-1}. (a) Discharge/charge profiles. (b) Cycling performance.*

DOI: 10.31635/ccschem.019.20190003
CCS Chem. **2019**, *1*, 365–372

bind with Li and Na (Supporting Information Figures S9–S13 and Tables S3 and S4). To confirm the calculation prediction, the electrochemical behavior of PoPD for LIBs and SIBs was examined (Figure 5 and Supporting Information Figures S4b,c and S14). After the initial activation process, PoPD delivered a reversible lithium storage capacity of 537 mAh·g^{-1} and sodium storage capacity of 307 mAh·g^{-1} even after the 300th cycle (Figure 5b, (Supporting Information Figures S15 and S16)), which provides convincing evidence for the broad practicability of this organic electrode material.

Conclusion

In summary, in response to the challenges of using an inorganic electrode for the reversible accommodation of different size metal ions, an imine-rich PoPD is obtained through a rational controllable oxidization, acting as a trifunctional electrode in alkali-ion batteries. Based on substantial characterization techniques and DFT calculations, PoPD with abundant active sites exhibits a stable cyclability at high capacity when acting as a PIB anode (450 mAh·g^{-1} after 205 cycles). At the same time, its successful application as a versatile electrode in lithium and sodium storage (537 and 307 mAh·g^{-1}after 300 cycles for LIBs and SIBs, respectively) extends the application range of PoPD and may even be useful for multivalent- and dual-ion batteries in the future. We anticipate that these findings will enlighten the design and application of organic electrode materials for cheap, green, sustainable, and versatile energy storage devices.

Supporting Information

Supporting information is available.

Conflicts of Interest

The authors declare no competing financial interests.

Acknowledgments

This work was financially supported by the National Natural Science Foundation of China (21725103 and 51472232), JCKY2016130B010, Jilin Province Science and Technology Development Plan Funding Project (20180101203JC and 20160101289JC), and Changchun Science and Technology Development Plan Funding Project (18DY012). T.S. and Z.J.L. contributed equally to this work.

References

1. Song, Z.; Zhou, H. Towards Sustainable and Versatile Energy Storage Devices: An Overview of Organic Electrode Materials. *Energy Environ. Sci.* **2013**, *6*, 2280–2301.
2. Wang, Y.; Chen, R.; Chen, T.; Lv, H.; Zhu, G.; Ma, L.; Wang, C.; Jin, Z.; Liu, J. Emerging Non-Lithium Ion Batteries. *Energy Storage Mater.* **2016**, *4*, 103–129.
3. Zhao, Q.; Lu, Y.; Chen, J. Advanced Organic Electrode Materials for Rechargeable Sodium-Ion Batteries. *Adv. Energy Mater.* **2016**, *7*, 1601792.
4. Wang, H.-G.; Yuan, S.; Ma, D.-L.; Huang, X.-L.; Meng, F.-L.; Zhang, X.-B. Tailored Aromatic Carbonyl Derivative Polyimides for High-Power and Long-Cycle Sodium-Organic Batteries. *Adv. Energy Mater.* **2014**, *4*, 1301651.
5. Lee, M.; Hong, J.; Kim, H.; Lim, H.-D.; Cho, S. B.; Kang, K.; Park, C. B. Organic Nanohybrids for Fast and Sustainable Energy Storage. *Adv. Mater.* **2014**, *26*, 2558–2565.
6. Chen, Y.; Luo, W.; Carter, M.; Zhou, L.; Dai, J.; Fu, K.; Lacey, S.; Li, T.; Wan, J.; Han, X.; Bao, Y.; Hu, L. Organic Electrode for Non-Aqueous Potassium-Ion Batteries. *Nano Energy* **2015**, *18*, 205–211.
7. Eftekhari, A.; Jian, Z.; Ji, X. Potassium Secondary Batteries. *ACS Appl. Mater. Interfaces* **2017**, *9*, 4404–4419.
8. Kim, H.; Kim, J. C.; Bianchini, M.; Seo, D. H.; Rodriguez-Garcia, J.; Ceder, G. Recent Progress and Perspective in Electrode Materials for K-Ion Batteries. *Adv. Energy Mater.* **2017**, *8*, 1702384.
9. Jian, Z.; Luo, W.; Ji, X. Carbon Electrodes for K-Ion Batteries. *J. Am. Chem. Soc.* **2015**, *137*, 11566–11569.
10. Jian, Z.; Xing, Z.; Bommier, C.; Li, Z.; Ji, X. Hard Carbon Microspheres: Potassium-Ion Anode Versus Sodium-Ion Anode. *Adv. Energy Mater.* **2016**, *6*, 1501874.
11. Luo, W.; Wan, J.; Ozdemir, B.; Bao, W.; Chen, Y.; Dai, J.; Lin, H.; Xu, Y.; Gu, F.; Barone, V.; Hu, L. Potassium Ion Batteries With Graphitic Materials. *Nano Lett.* **2015**, *15*, 7671–7677.
12. Zhao, J.; Zou, X.; Zhu, Y.; Xu, Y.; Wang, C. Electrochemical Intercalation of Potassium Into Graphite. *Adv. Funct. Mater.* **2016**, *26*, 8103–8110.
13. Zhang, W.; Mao, J.; Li, S.; Chen, Z.; Guo, Z. Phosphorus-Based Alloy Materials for Advanced Potassium-Ion Battery Anode. *J. Am. Chem. Soc.* **2017**, *139*, 3316–3319.
14. Sultana, I.; Ramireddy, T.; Rahman, M. M.; Chen, Y.; Glushenkov, A. M. Tin-Based Composite Anodes for Potassium-Ion Batteries. *Chem. Commun.* **2016**, *52*, 9279–9282.
15. Han, J.; Niu, Y.; Bao, S.-J.; Yu, Y.-N.; Lu, S.-Y.; Xu, M. Nanocubic $KTi_2(PO_4)_3$ Electrodes for Potassium-Ion Batteries. *Chem. Commun.* **2016**, *52*, 11661–11664.
16. Kishore, B.; Venkatesh, G.; Munichandraiah, N. $K_2Ti_4O_9$: A Promising Anode Material for Potassium Ion Batteries. *J. Electrochem. Soc.* **2016**, *163*, A2551–A2554.
17. Ren, X.; Zhao, Q.; McCulloch, W. D.; Wu, Y. MoS_2 as a Long-Life Host Material for Potassium Ion Intercalation. *Nano Res.* **2017**, *10*, 1313–1321.
18. Jian, Z.; Liang, Y.; Rodríguez-Pérez, I. A.; Yao, Y.; Ji, X. Poly(anthraquinonyl sulfide) Cathode for Potassium-Ion Batteries. *Electrochem. Commun.* **2016**, *71*, 5–8.
19. Deng, Q.; Pei, J.; Fan, C.; Ma, J.; Cao, B.; Li, C.; Jin, Y.; Wang, L.; Li, J. Potassium Salts of Para-Aromatic Dicarboxylates as the Highly Efficient Organic Anodes for Low-Cost K-Ion Batteries. *Nano Energy* **2017**, *33*, 350–355.
20. Lei, K.; Li, F.; Mu, C.; Wang, J.; Zhao, Q.; Chen, C.; Chen, J. High K-Storage Performance Based on the Synergy of

DOI: 10.31635/ccschem.019.20190003
CCS Chem. **2019**, *1*, 365–372

Dipotassium Terephthalate and Ether-Based Electrolytes. *Energy Environ. Sci.* **2017**, *10*, 552–557.
21. Xing, Z.; Jian, Z.; Luo, W.; Qi, Y.; Bommier, C.; Chong, E. S.; Li, Z.; Hu, L.; Ji, X. A Perylene Anhydride Crystal as a Reversible Electrode for K-Ion Batteries. *Energy Storage Mater.* **2016**, *2*, 63–68.
22. Muench, S.; Wild, A.; Friebe, C.; Häupler, B.; Janoschka, T.; Schubert, U. S. Polymer-Based Organic Batteries. *Chem. Rev.* **2016**, *116*, 9438–9484.
23. Zhao, R.; Zhu, L.; Cao, Y.; Ai, X.; Yang, H. X. An Aniline-Nitroaniline Copolymer as a High Capacity Cathode for Na-Ion Batteries. *Electrochem. Commun.* **2012**, *21*, 36–38.
24. Li, X.-G.; Huang, M.-R.; Duan, W.; Yang, Y.-L. Novel Multifunctional Polymers From Aromatic Diamines by Oxidative Polymerizations. *Chem. Rev.* **2002**, *102*, 2925–3030.
25. Li, X.-G.; Ma, X.-L.; Sun, J.; Huang, M.-R. Powerful Reactive Sorption of Silver(I) and Mercury(II) Onto Poly(*o*-phenylenediamine) Microparticles. *Langmuir* **2009**, *25*, 1675–1684.
26. Sun, T.; Li, Z. J.; Wang, H. G.; Bao, D.; Meng, F. L.; Zhang, X. B. A Biodegradable Polydopamine-Derived Electrode Material for High-Capacity and Long-Life Lithium-Ion and Sodium-Ion Batteries. *Angew. Chem. Int. Ed.* **2016**, *55*, 10662–10666.
27. Yang, A.; Wang, X.; Lu, Y.; Miao, L.; Xie, W.; Chen, J. Core-Shell Structured 1,4-Benzoquinone@TiO_2 Cathode for Lithium Batteries. *J. Energy Chem.* **2018**, *27*, 1644–1650.
28. Lu, Y.; Zhang, Q.; Li, L.; Niu, Z.; Chen, J. Design Strategies Toward Enhancing the Performance of Organic Electrode Materials in Metal-Ion Batteries. *Chem* **2018**, *4*, 2786–2813.
29. Wu, J.; Rui, X.; Long, G.; Chen, W.; Yan, Q.; Zhang, Q. Pushing Up Lithium Storage Through Nanostructured Polyazaacene Analogues as Anode. *Angew. Chem. Int. Ed.* **2015**, *54*, 7354–7358.
30. Kim, K. C.; Liu, T.; Lee, S. W.; Jang, S. S. First-Principles Density Functional Theory Modeling of Li Binding: Thermodynamics and Redox Properties of Quinone Derivatives for Lithium-Ion Batteries. *J. Am. Chem. Soc.* **2016**, *138*, 2374–2382.
31. Lee, M.; Hong, J.; Seo, D. H.; Nam, D. H.; Nam, K. T.; Kang, K.; Park, C. B. Redox Cofactor From Biological Energy Transduction as Molecularly Tunable Energy-Storage Compound. *Angew. Chem. Int. Ed.* **2013**, *52*, 8322–8328.
32. Lee, H. H.; Park, Y.; Shin, K.-H.; Lee, K. T.; Hong, S. Y. Abnormal Excess Capacity of Conjugated Dicarboxylates in Lithium-Ion Batteries. *ACS Appl. Mater. Interfaces* **2014**, *6*, 19118–19126.

DOI: 10.31635/ccschem.019.20190003
CCS Chem. **2019**, *1*, 365–372